Changes in Nanoscale Porosity by Wet Pressing Pulps from Sugarcane Bagasse

Marcelo M. Oliveira,[a,b] Carlos Driemeier,[b] and Antonio A. S. Curvelo [b,c,*]

Nanoscale porosity is critical for cellulose reactivity and can be detrimentally affected by wet pressing. The present study evaluated how wet pressing reduced the nanoscale porosity of a set of pulps produced from sugarcane bagasse. The pulps were produced using hydrothermal treatments, followed by either 160 °C alkaline (sodium hydroxide) or 190 °C organosolv (ethanol-water) pulping. Pulping times (20, 40, 60, 80, and 100 min) and applied pressures in the pressing step (21, 43, 64, 85, and 107 MPa) were varied, and the resulting samples had their nanoscale porosity characterized using calorimetric thermoporometry. The lowest applied pressure (21 MPa) collapsed a considerable fraction of the nanoscale porosities. Otherwise, when additional pressure (up to 107 MPa) was applied, a much lower reduction in porosity was observed. The findings indicate that nanoscale porosity of pulps can be separated into compressible and incompressible components.

Keywords: Biomass; Sugarcane bagasse; Lignocellulosic; Porosity; Thermoporometry; Wet pressing

Contact information: a: Escola de Engenharia de São Carlos (EESC), Universidade de São Paulo (USP), Caixa Postal:780, 13560-970, São Carlos, São Paulo, Brasil; b: Laboratório Nacional de Ciência e Tecnologia do Bioetanol (CTBE), Centro Nacional de Pesquisas em Energia e Materiais (CNPEM), Caixa Postal: 6192, 13083-970, Campinas, São Paulo, Brasil; c: Instituto de Química de São Carlos (IQSC), Universidade de São Paulo (USP), Caixa Postal: 780, 13560-970, São Carlos, São Paulo, Brasil;
** Corresponding author: aprigio@iqsc.usp.br*

INTRODUCTION

Lignocellulosic biomass is a vast renewable feedstock for the production of materials, chemicals, and liquid biofuels. Sugarcane bagasse is one especially attractive type of lignocellulosic feedstock because it is available on-site as an abundant underutilized residue of sugar-ethanol mills (Cortez 2010). With such potential, intense research and development have been dedicated towards developing cost-effective processes to convert sugarcane bagasse into value-added products.

Chemical reactions for the deconstruction of lignocellulosic biomass depend on the transport of reactants, catalysts, and reaction products inside the porous structure of the biomass. Porosity includes the micrometric pores originating from the interior (lumen) of plant cells, as well as nanoscale pores within the cell walls (Stone and Scallan 1968; Fahlén and Salmén 2005; Maziero *et al.* 2013). Specific surface areas associated with nanometric pores are a few orders of magnitude greater than specific areas because of micrometric pores and external particle surfaces (Driemeier *et al*. 2011; Bragatto *et al*. 2012). Therefore, nanoscale porosity is often critical for biomass chemical reactivity. In particular, enzymatic saccharification of cellulose is critically affected by nanoscale porosity. This is because enzymes are approximately 5 nm in size, requiring pores larger than that for enzyme penetration into the walls, thus enabling extensive cellulose saccharification.

Lignocellulose nanoscale porosity is influenced by many factors. As a starting point, nanoscale porosity depends on plant tissue and its maturity (Maziero *et al*. 2013). Chemical treatments, such as pulping or hydrothermal treatments performed prior to enzymatic digestion, usually increase nanoscale porosity (Stone and Scallan 1968; Fahlén and Salmén 2005; Ishizawa *et al*. 2007), in addition to mechanical disintegration processes (Fahlén and Salmén 2005; Grönqvist *et al*. 2014; Wang *et al*. 2014). On the other hand, pressing and drying reduces nanoscale porosity (Maloney *et al.* 1997; Haggkvist *et al.* 1998; Park *et al.* 2006; Luo *et al*. 2011; Pönni *et al.* 2012).

The collapse of nanoscale pores because of drying implies that wet methods are required to characterize biomass nanoscale porosity in a state representative of aqueous processing. One such method is thermoporometry, which is based on the temperature depression of the ice-water phase transition occurring under nanometric confinement (Brun *et al*. 1977; Petrov and Furó 2009). The ice melting transition can be detected by nuclear magnetic resonance (Ishizawa *et al*. 2007; Petrov and Furó 2009), as well as by differential scanning calorimetry (Brun *et al*. 1977; Maloney and Paulapuro 1999; Park *et al*. 2006; Driemeier *et al.* 2012). Thermoporometry analysis of cellulosic biomass determines the pore size distributions in the 1 to 400 nm range.

This article investigates how cellulosic pulps, obtained from sugarcane bagasse, are modified in nanoscale porosity using the wet pressing technique. Wet pressing is potentially beneficial to biomass conversion economics because of the higher solid loading potential in the reactors. On the other hand, wet pressing is also potentially detrimental to processing because of the particulate compaction and loss of biomass porosity. By employing thermoporometry to characterize nanoscale porosity after different pulping and pressing conditions, this article contributes to the understanding of how wet pressing affects the nanoscale porosity of cellulosic pulps.

EXPERIMENTAL

Sugarcane Bagasse

Sugarcane bagasse was provided by Usina Ipiranga de Açúcar e Álcool Ltda, located in Descalvado, São Paulo, Brazil. Bagasse was washed in hot (70 °C) water in order to remove residual sucrose. Granulometric fractionation of bagasse was performed using a column of sieves of 16, 60, and 250 mesh (1.18; 0.250, and 0.063 mm, respectively). Fractions retained on the sieves of 16 and 60 mesh were rich in bagasse fibrous particles. These two fractions were mixed, homogenized, and then used in the following procedures.

Chemical Fractionation

Bagasse chemical fractionation was performed in two sequential steps. The first step was a hydrothermal treatment performed at 160 °C for 30 min with approximately 13 L of water and 1.3 kg (dry mass) of solid, in an electronic autoclave system (REGMED model AU/20). After the reaction, the solid fraction was washed with water. The hydrothermally-treated solid was subjected to a second chemical fractionation step of either organosolv or alkaline pulping. Both delignification reactions were performed with a solid-liquid ratio of 1:10 (w/v) in a 200 mL custom-built steel reactor, which was heated using a glycerin thermostatic bath with mechanical stirring and a digital temperature control. The reaction temperatures were set to 190 °C (organosolv) and 160 °C (alkaline). The organosolv liquid was a 50/50 (v:v), ethanol-water mixture. The alkaline liquid was an

aqueous solution of 20% sodium hydroxide with 0.15% anthraquinone catalyst. Reaction times were 20, 40, 60, 80, and 100 min. Reactions began with the immersion of the reactors into the thermostatic bath (already at target temperature) and was stopped by immersion in an ice bath. After cooling, reactor contents were subjected to a defiber process with a solution of 1.0% sodium hydroxide to remove any absorbed lignin on the cellulosic fibers. Afterwards, the cellulosic pulps were washed with distilled water until the pH of the washing water remained unaltered.

Solubilization

Solubilization was defined as the percentage of dry mass removed from the solid into the solution during the delignification process. Solubilization was determined gravimetrically by measuring the initial (m_i) and final (m_f) masses of the solid submitted by delignification (Eq. 1). Determination of m_i and m_f accounted for sample moisture content, as determined by a thermobalance (TopRay series, Bel Engineering, Piracicaba, Brazil):

$$S = \left(1 - \frac{m_f}{m_i}\right) \times 100 \quad (1)$$

Wet Pressing

Wet pressing was performed in a hydraulic press (Nowak, São Jose do Rio Preto, Brazil) with a nominal maximum load of 30 tons. A custom-built wet compression cell was made on polished 304 steel (Fig. 1).

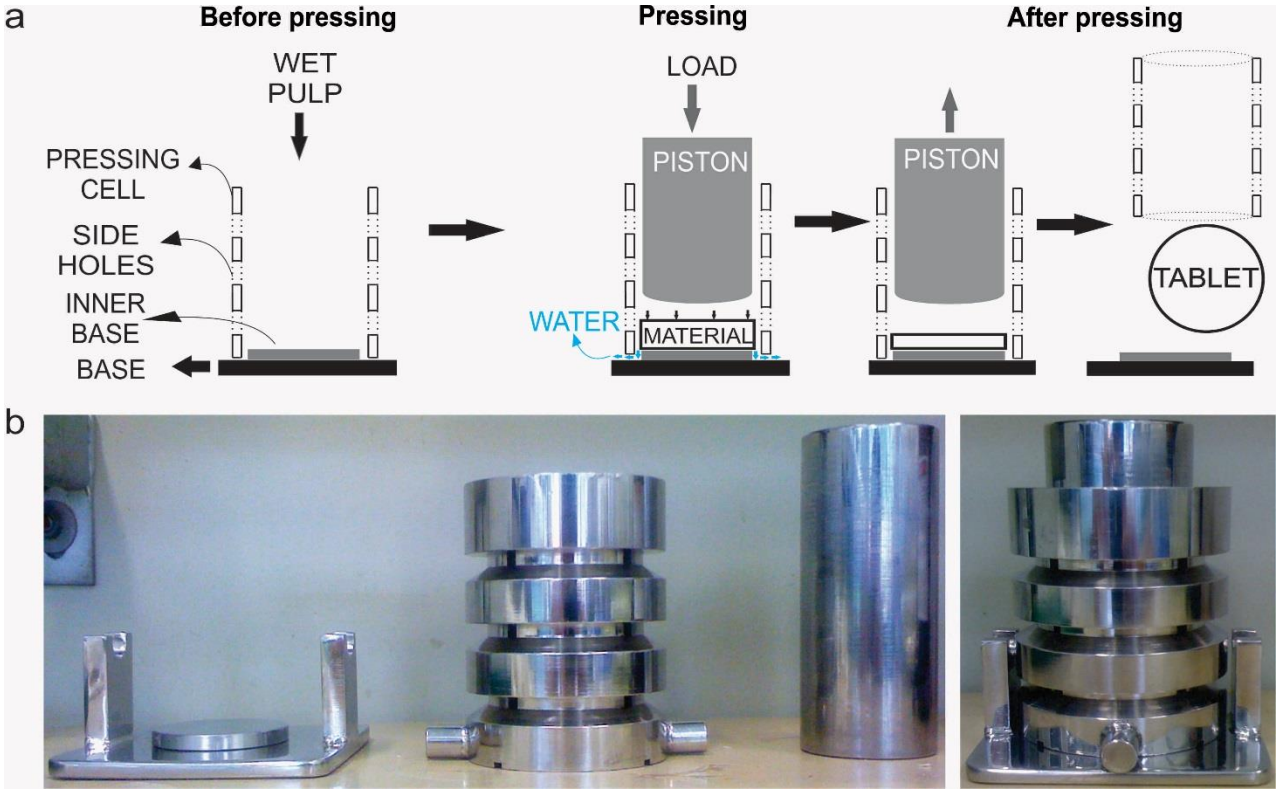

Fig. 1. System used for wet pressing: a) Sketch of a wet pressing test, b) Images of the disassembled (left) and assembled (right) compression cell

Each pressing test employed 1.5 g (dry basis) of wet pulp (over 60% humidity) homogeneously distributed at the base of the cylindrical compression cell (54 mm of internal diameter). Wet pulp was then slowly compressed using a cylindrical piston of the same diameter. The load was maintained for 5 min after reaching the target load. Loads of 5, 10, 15, 20, and 25 tons were applied, corresponding to pressures of 21, 43, 64, 85, and 107 MPa, respectively. During compression, liquid was expelled through four radial holes of 5 mm diameter, located at the base and lateral sides of the cylindrical compression cell. Figure 1 shows a sketch of wet pressing and images of the compression cell. Pressed pulps formed tablets, which were stored at 5 °C in sealed containers prior to characterization of nanoscale porosity.

X-Ray Diffraction

X-ray diffraction was performed in transmission geometry with air-dried powdered specimens conditioned in capillary tubes. Two-dimensional diffraction patterns were recorded using a mar345 image plate, with calibration and intensity correction as detailed elsewhere (Driemeier and Calligaris 2011). This detection system was coupled to the MX1 beamline of the Brazilian Synchrotron Light Laboratory (Polikarpov *et al*. 1998), with X-ray wavelength set to 1.4535 Å. Note that this wavelength differs from the usual CuKα sources (1.54 Å), so that the diffraction peaks would appear in different scattering angles 2θ.

Thermoporometry

Nanoscale porosity was evaluated through thermoporometry using differential scanning calorimetry (DSC). Measurements were carried out in a TA Q200 instrument with RCS90 cooling system (TA Instruments, New Castle, USA). A steel punch (3 mm diameter) was used to collect samples from the compressed tablets. The wet samples were conditioned by immersion in deionized water for 24 h prior to insertion into the DSC Tzero® aluminum pans with hermetic lids.

As the first step of each DSC analysis, the sample was frozen at -70 °C. Then, the temperature was increased stepwise to 5 °C. Each heating step was comprised of a ramp followed by a stabilization isotherm. The calorimetric signal of ice melting below 0 °C was attributed to water confined in nanoscale pores, also known as freezing bound water (FBW). The temperature depression (ΔT) of ice melting was related to pore diameter (d) according to the Gibbs-Thomson equation, $d = 2\ K_c\ /\ \Delta T$, where $K_c = 19.8$ nm K. The calorimetric signal was converted to FBW (in units of water g per dry matter g) as a cumulative distribution function of d, as detailed elsewhere (Driemeier *et al*. 2012).

Regression Analysis

The thermoporometry data of the pressed pulps was analyzed by linear regression. The FBW at a given pore diameter was modeled as the sum of a constant (C_0), a term proportional to applied pressure (P), and another term proportional to solubilization (S), as follows (Eq. 2),

$$\mathrm{FBW} = C_0 + (C_S \times S) + (C_P \times P) \quad (2)$$

where, C_0, C_S, and C_P were determined by fitting the experimental data according to matrix algebra (Rencher 2003).

RESULTS AND DISCUSSION

The pulping processes solubilized variable fractions of the prehydrolyzed solid. For both the alkaline and organosolv delignification, the trend of solubilization increased with increasing treatment time. This trend was most likely caused by the progressive removal of biomass components, mainly lignin, as the treatment time was increased. An exception was the alkaline process at the longest treatment time (100 min), which exhibited a lower solubilization than the 80 min process. This exception was perhaps a result of lignin deposition on the surface of the material over a long treatment time. Table 1 shows the value of solubilization means ± the standard deviation of the duplicates.

Table 1. Percent Solubilization in Different Delignification Conditions

Treatment time (min)	Solubilization (%)	
	Alkaline	Organosolv
20	42.9 ± 0.1	18.8 ± 0.9
40	56.1 ± 0.3	23.1 ± 0.1
60	59.7 ± 1.4	27.7 ± 1.3
80	63.3 ± 0.3	33.3 ± 0.4
100	57.4 ± 0.2	38.9 ± 0.5

The unpressed pulps were characterized using X-ray diffraction. Organosolv pulps exhibited diffractograms characteristic of the native phase cellulose I, while alkaline pulps presented the characteristic features of cellulose II (Fig. 2). These findings indicate that the alkaline pulping conditions promoted cellulose mercerization, converting cellulose I into cellulose II. In addition to diffraction peaks from cellulose, minor and sharper peaks were observed at $2\theta \approx 27°$ (organosolv), as well as at ≈24° and ≈25° (alkaline). These minor peaks arose from unidentified crystalline contaminants.

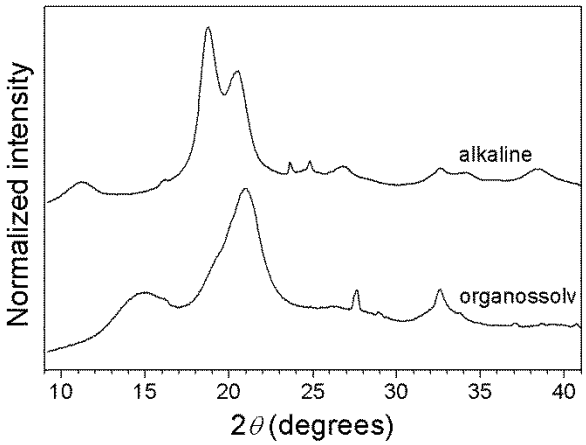

Fig. 2. Diffractograms of pulps produced by alkaline and organossolv treatments (reaction time of 60 min), showing the typical patterns of cellulose II and cellulose I, respectively

The wet pressing of alkaline and organosolv pulps produced nonhomogeneous tablets, with the center of each tablet denser than its borders. This inhomogeneity resulted from the geometry of the pressing cell (Fig. 1). Figure 3 shows pulps before and after wet pressing. The alkaline pulps are whiter because more lignin was removed, as compared to the organosolv pulps. The size of the samples collected for thermoporometry is also indicated in the images below.

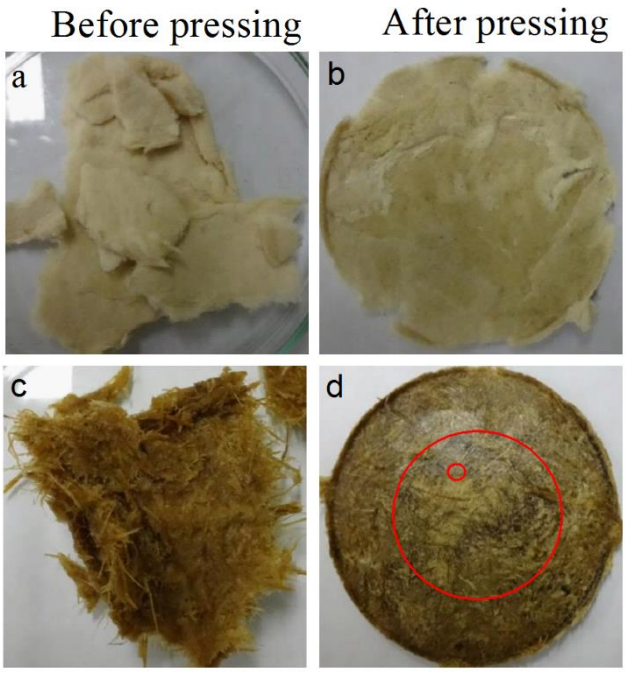

Fig. 3. Images taken of alkaline (a and b) and organosolv (c and d) pulps before and after wet pressing. The materials shown in the images were pulped for 20 min and pressed at 107 MPa. The circles in (d) have diameters of 3 cm and 3 mm, respectively, corresponing to the region considered for sampling and the actual size of one sample selected for thermoporometry analysis

The thermoporometry measurements of the pulps before and after wet pressing exhibited a reduction in nanoscale porosity at every applied pressure (Fig. 4).

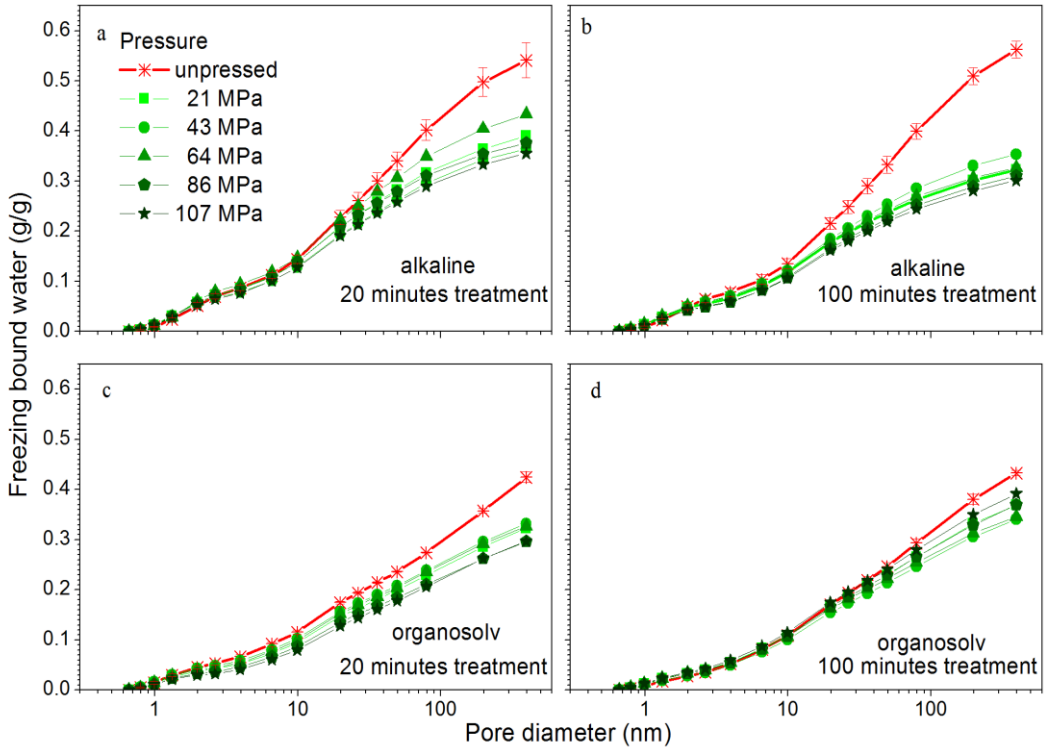

Fig. 4. Results of thermoporometry for alkaline (a and b) and organossolv (c and d) pulps, produced with 20 min (a and c) and 100 min (b and d) pulping times, before and after wet pressing at different pressures

Note that the presented profiles are cumulative distributions of FBW, presented as a function of pore diameter in log scale. The reduction in porosity resulted from pressing that occurred mostly for pores greater than 20 nm in diameter. Moreover, the degree of porosity reduction varied between alkaline and organosolv pulps, with the alkaline pulps showing more pronounced porosity reduction. The greater susceptibility to wet pressing of alkaline pulps may have resulted in greater solubilization (Table 1), cellulose phase change (Fig. 2), or swelling left by the alkali processing. Figure 4 shows the thermoporometry profiles for alkaline and organosolv pulps of two treatment times (20 and 100 min). For each type of pulping, the porosity of the pressed pulps was not significantly different as experimental uncertainty was considered.

By regression analysis, finer information can be obtained concerning sample differences and trends associated with solubilization and applied pressures. Instead of comparing individual thermoporometry curves, sets of curves were jointly analyzed. The line of best fit for the curves were performed using Eq. 2, applied separately to the compressed pulps produced by either alkaline or organosolv treatments. Figure 5 compares experimental and calculated regression data, showing remarkable agreement between alkaline (R^2 = 0.987) and organosolv pulp (R^2 = 0.995). Except for a very low FBW, relative residues (Fig. 5c and 5d) were mostly within 20%. This is the expected range of residues given the experimental uncertainties.

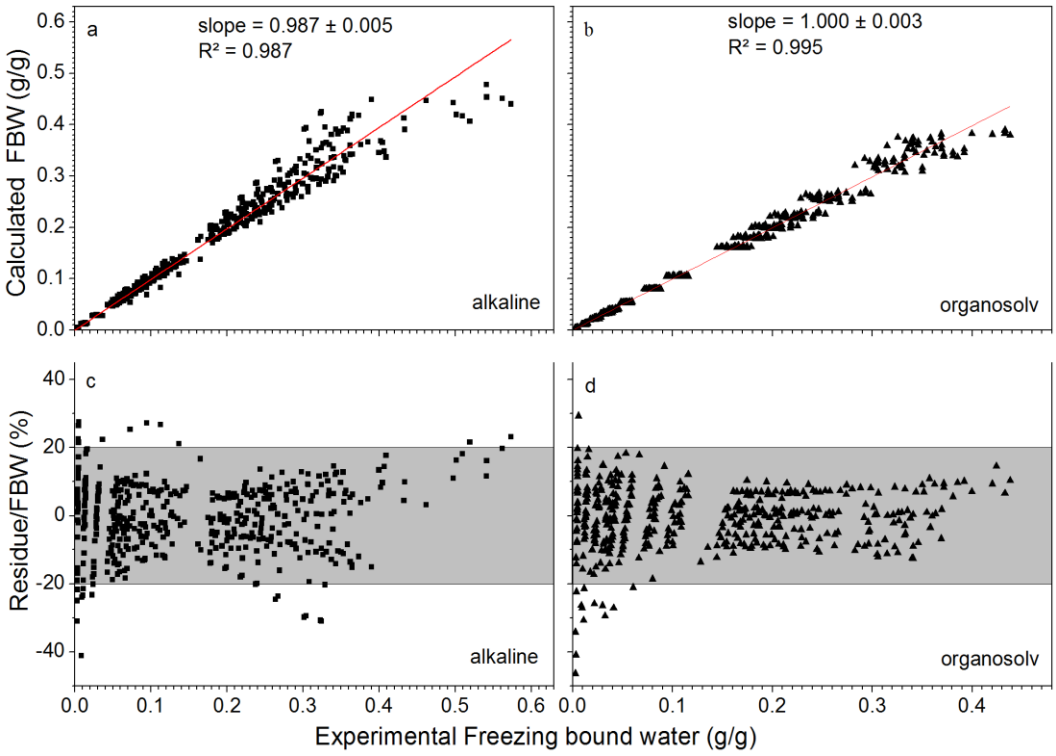

Fig. 5. Validation of linear regression of thermoporometry profiles for alkaline (a and c) and organosolv pulps (b and d)

The coefficients obtained from the linear regressions are shown in Fig. 6. Non-zero coefficients, C_s and C_p, were observed, revealing roles of solubilization and pressure in the resulting nanoscale porosities. Negative C_p coefficients for both alkaline and organosolv pulps demonstrated that the applied pressure reduced nanoscale porosity, especially for

pores that were greater than 20 nm in diameter. However, the reduction observed across compressed pulps was minor (Fig. 6) in comparison to the reduction in porosity of unpressed pulps (Fig. 4). Solubilization, on the other hand, presented either positive (organosolv) or negative (alkaline) C_S coefficients (Fig. 6). This result revealed that higher solubilization may lead to either higher or lower nanoscale porosities, depending on the type of the pulping process. The coefficient, C_0, can be interpreted as the FBW extrapolated to zero solubilization and pressure, where only data from pressed pulps were used for the extrapolation. The alkaline pulps presented greater C_0 coefficients than the organosolv pulps. This result rejects the aforementioned hypothesis that higher porosity results from higher solubilization in alkaline pulps (Table 1). Hence, the higher porosity of the alkaline pulps can be attributed either to cellulose phase change (Fig. 2) or the swelling power of the alkali.

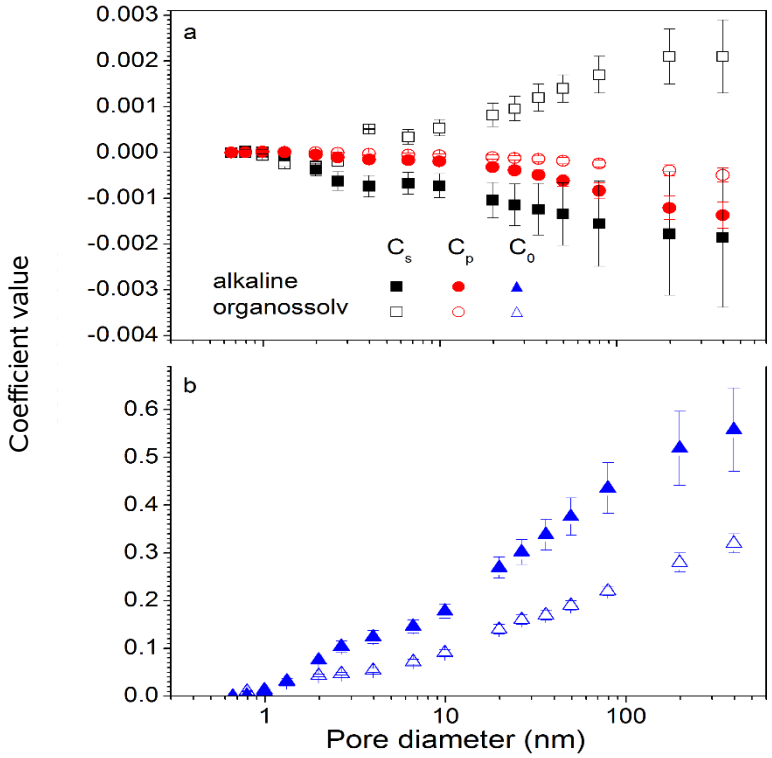

Fig. 6. Coefficients from linear regression of thermoporometry data of pressed pulps. Solubilization and pressure coefficients (C_s and C_p, respectively) are shown in a, while the coefficient C_0 is shown in b. The coefficients C_s, C_p, and C_0 are calculated for every pore diameter recorded in the thermoporometry profiles

CONCLUSIONS

1) This study employed calorimetric thermoporometry to evaluate the wet nanoscale porosities of cellulose pulps produced from sugarcane bagasse and submitted to wet pressing.
2) Two types of pulps were investigated: organosolv (ethanol-water) pulp, which retained the native cellulose I crystal phase, and alkaline (NaOH) pulp, which showed a conversion to cellulose II.

3) Both the organosolv and alkaline pulps resulted in nanoscale porosity reduction caused by wet pressing. The more substantial reduction was observed in response to the lowest applied pressure (21 MPa). Higher pressures (up to 107 MPa) promoted additional porosity reduction; however, this reduction was marginal and still left significant remaining porosities.
4) The results indicated that the wet nanoscale porosities of pulps can be separated into two components: compressible and mostly incompressible.

ACKNOWLEDGMENTS

The authors would like to thank Usina Ipiranga de Açúcar e Álcool Ltda for kindly providing the sugarcane bagasse, Fernanda M. Mendes for helping with the thermoporometry measurements, São Paulo Research Foundation (FAPESP) for the scholarship (grant 2011/14746-9) and National Council for Scientific and Technological Development (CNPq) and National Council for the Improvement of Higher Education (CAPES) for their financial support.

REFERENCES CITED

Bragatto, J., Segato, F., Cota, J., Mello, D. B, Oliveira, M. M., Buckeridge, M. S., Squina, F. M., Driemeier, C. (2012). "Insights on how the activity of an endoglucanase is affected by physical properties of insoluble celluloses," *J. Phys. Chem. B* 116(21), 6128-6136. DOI: 10.1021/jp3021744

Brun, M., Lallemand, A., Quinson, J. F., and Eyraud, C. (1977). "A new method for the simultaneous determination of the size and shape of pores: The thermoporometry," *Thermochim. Acta.* 21(1), 59-88. DOI: 10.1016/0040-6031(77)85122-8

Cortez, L. A. B. (2010). "Sugar cane bioethanol: R&D for productivity and sustainability," 1st Edition, Blucher, São Paulo. DOI: 10.5151BlucherOA-Sugarcane. Blucher.

Driemeier, C., and Calligaris, G. A. (2011). "Theoretical and experimental developments for accurate determination of crystallinity of cellulose I materials," *J. Appl. Crystal.* 44(1), 184-192. DOI: 10.1107/S0021889810043955

Driemeier, C., Mendes, F. M., and Oliveira, M. M. (2012). "Dynamic vapor sorption and thermoporometry to probe water in celluloses," *Cellulose* 19(4), 1051-1063. DOI: 10.1007/s10570-012-9727-z

Driemeier, C., Oliveira, M. M., Mendes, F. M., and Gómez, E. O. (2011). "Characterization of sugarcane bagasse powders," *Powder Technol*. 214(1), 111-116. DOI: 10.1016/j.powtec.2011.07.043

Fahlén, J., and Salmén, L. (2005). "Pore and matrix distribution in the fiber wall revealed by atomic force microscopy and image analysis," *Biomacromol.* 6(1), 433-438. DOI: 10.1021/bm040068x

Grönqvist, S., Hakala, T. K., Kamppuri, T., Vehviläinen, M., Hänninen, T., Liitiä, T., Maloney, T., Suurnäkki, A. (2014). "Fibre porosity development of dissolving pulp during mechanical and enzymatic processing," *Cellulose* 21(5), 3667-3676. DOI: 10.1007/s10570-014-0352-x

Haggkvist, M., Li, T-Q., and Odberg, L. (1998). "Effects of drying and pressing on the pore structure in the cellulose fibre wall studied by 1H and 2H NMR relaxation," *Cellulose* 5(1), 33-49. DOI: 10.1023/A:1009212628778

Ishizawa, C. I., Davis, M. F., Schell, D. F., and Johnson, D. K. (2007). "Porosity and its effect on the digestibility of dilute sulfuric acid pretreated corn stover," *J. Agric. Food Chem.* 55(7), 2575-2581. DOI: 10.1021/jf062131a

Luo, X. L., Zhu, J. Y., Gleisner, R., and Zhan, H. Y. (2011). "Effects of wet-pressing-induced fiber hornification on enzymatic saccharification of lignocelluloses," *Cellulose* 18(4), 1055-1062. DOI: 10.1007/s10570-011-9541-z

Maloney, T. C., Tie-Qiang, L., Weise, U., and Paulapuro, H. (1997). "Intra- and inter-fibre pore closure in wet pressing," *APPITA Journal* 50(4), 301-306.

Maloney, T. C., and Paulapuro, H. (1999). "The formation of pores in the cell wall," *J. Pulp. Pap. Sci.* 25(12), 430-436.

Maziero, P., Jong, J., Mendes, F. M., Gonçalves, A. R., Eder, M., Driemeier, C. (2013). "Tissue-Specific cell wall hydration in sugarcane stalks," *J. Agric. Food. Chem.* 61(24), 5841-5847. DOI: 10.1021/jf401243c

Park, S., Venditti, R. A., Jameel, H., and Pawlak, J. J. (2006). "Changes in pore size distribution during the drying of cellulose fibers as measured by differential scanning calorimetry," *Carbohydr. Polym.* 66(1), 97-103. DOI: 10.1016/j.carbpol.2006.02.026

Petrov, O. V., and Furó, I. (2009). "NMR cryoporometry: Principles, applications and potential," *Prog. Nucl. Magn. Reson. Spectrosc.* 54(2), 97-122. DOI: 10.1016/j.pnmrs.2008.06.001

Polikarpov, I., Perles, L. A., De Oliveira, R. T., Oliva, G., Castellano, E. E., Garratt, R. C., and Craievich, A. (1998). "Set-up and experimental parameters of the protein crystallography beamline at the Brazilian National Synchrotron Laboratory," *J. Synch. Rad.* 5(2), 72-76. DOI: 10.1107/S0909049597014684

Pönni, R., Vuorinen, T., and Kontturi, E. (2012). "Proposed nano-scale coalescence of cellulose in chemical pulp fibers during technical treatments," *BioResources* 7(4), 1-32. DOI: 10.15376/biores.7.4.6077-6108

Rencher, A. C. (2003). "Multivariate regression," *Methods of Multivariate Analysis*, 2nd Edition, John Wiley & Sons Inc., New York. DOI: 10.1002/0471271357.ch10

Stone, J. E., and Scallan, A. M. (1968). "A structural model for the cell wall of water-swollen wood pulp fibres based on their accessibility to macromolecules," *Cell. Chem. Technol.* 2(3), 343-358.

Wang, W., Chen, X., Donohoe, B. S., Ciesielski, P. N., Katahira, R., Kuhn, E. M., Kafle, K., Lee, C. M., Park, S., Kim, S. H., Tucker, M. P., Himmel, M. E., and Johnson, D. K. (2014). "Effect of mechanical disruption on the effectiveness of three reactors used for dilute acid pretreatment of corn stover Part 1: chemical and physical substrate analysis," *Biotechnol. Biofuels* 7(1), 57. DOI: 10.1186/1754-6834-7-57

Article submitted: August 4, 2015; Peer review completed: October 5, 2015; Revised version received and accepted: October 12, 2015; Published: November 3, 2015.
DOI: 10.15376/biores.10.4.8518-8527